Semi-Analytical Weight Estimation Method for Fuselages with Oval Cross-Section

Roelof Vos* and Maurice Hoogreef†
Delft University of Technology, Delft, The Netherlands

This paper presents a semi-analytical method for the weight estimation of fuselages with an oval cross-section, applied to blended wing body aircraft. The weight estimation of the fuselage primary structure is based on a structural analysis of two-dimensional cross-sections and it is completed by a set of empirical relations for the weight estimation of the secondary structure and non-structural items. A conceptual design study on a stable (5% static margin), 400-passenger blended wing body aircraft has been performed with the weight estimation method implemented in an aircraft conceptual-design program. A top level requirement for the harmonic range of 15,200km was imposed on the design. From the anaylis a maximum take-off weight of 395 metric tons has been found, with an operative empty weight fraction of 45% and a fuselage airframe weight of 47.3 metric tons (amounting to 26% of the operative empty weight). The results of this study are presented in comparison to the Boeing 777-200LR airliner, showing a slightly higher operative empty weight fraction, a lower fuel consumption of 2.05kg per passenger per 100km.

List of Symbols

A_1	Ceiling structural half width, [m]
A_2	Floor structural half width, [m]
A_{1_c}	Ceiling cabin half width, [m]
A_{2_c}	Floor cabin half width, [m]
B	Wall structural length, [m]
b	Length of an unsupported member, [m]
C_{l_β}	Effective dihedral, [1/rad]
C_{n_β}	Weathercock stability, [1/rad]
c	Chord, [m]
d	Cross-section spacing, [m]
E	Young's Modulus, [N/m^2]
F	Force, [N]
$\bar{f}_t$	Ratio of working stress to 10^8, [-]
h	Structural cabin height, [m]
h_c	Factor for bulkhead shape, [-]
$\bar{h}$	Structural cabin height, [m]
I	Second moment of area, [m^4]
j	Safety factor, [-]
K_{door}	Factor accounting for cut-outs, [-]
K_{lg}	Factor accounting for landing gear attachments, [-]
m	Mass, [kg]
M	Bending moment, [Nm]
n	Load factor [-]
R	Radius, [m]
S	Surface area, [m^2]
t	Thickness, [m]
$\bar{t}$	Equivalent thickness, [m]
V_D	Dive speed, [m/s]
W	Weight, [kg]
x_{ac}	x-location of aerodynamic center, [m]
x_{cg}	x-location of center of gravity, [m]
Δ	Factor accounting for flap type, [-]
Δl	Unit length, [m]
Δp	Pressure differential, [N/m^2]
ρ	Density, [kg/m^3]
$\sigma_{fatigue_t}$	Tensile limit fatigue stress, [N/m^2]

Subscripts

1	Upper arc
2	Side arc
3	Lower arc
c	Core
cf	Crew floor
ceiling	Ceiling
crit	Critical
eng	Engine
f	Facing
floor	Floor
fpb	Front pressure bulkhead

*Assistant Professor, Faculty of Aerospace Engineering, Kluyverweg 1, 2629 HS Delft, The Netherlands, AIAA member
†PhD Candidate, Faculty of Aerospace Engineering, Kluyverweg 1, 2629 HS Delft, The Netherlands, AIAA student member

frf	Freight floor
fuel	Fuel
fus_{TE}	Fuselage trailing edge
h	Horizontal component
i	Index number
L	Lift
mat	Material
N_{ult}	Ultimate load factor
nc	Nose cone
paint	Paint
res	Resultant
rpb	Rear pressure bulkhead
shell	Shell
TE	Trailing edge
TO	Take-off
t	Top member
top	Top member
WS	Wind screen
wall	Wall
wet	Wetted area

I. Introduction

The blended-wing-body (BWB) aircraft has been under scrutiny by academia and industry for almost 20 years. Aerodynamic analysis has demonstrated that this vehicle could have a cruise lift-to-drag ratio in excess of 25. Furthermore, scale model tests have also shown that the handling characteristics of such a vehicle are acceptable. These characteristics would make the BWB an excellent candidate to replace the fleets of conventional wide-bodies, were it not for a few fundamental drawbacks of this concept. Many of these drawbacks stem from the integrated cabin. It has less windows, evacuation is more difficult, and the non-circular cross-section leads to a low structural efficiency.

Two main concepts in the open literature appear to carry the pressurization loads in a BWB aircraft. The first concept integrates the outer skin with the cabin (Fig. 1(a)). To maintain the non-circular shape, the upper and lower skin of the body are connected through vertical pillars. The shell in between the pillars is made from a sandwich structure, which carries the pressurization loads in bending.[1] The second concept segregates the aerodynamic outer skin from the pressure cabin (Fig. 1(b)). The cabin is formed by a set of intersecting circular tubes, which are connected through vertical members (pillars or walls). This concept has the advantage that upon pressurization the entire cabin structure is under tensile stress, which allows for a more efficient structure than the integrated concept.[2]

One of the most fundamental drawbacks of both concepts is the interruption of the open cabin space by vertical pillars or walls to ensure that the cabin maintains its shape upon pressurization. If walls are positioned, they prohibit natural light from the already scarce number of windows to travel throughout the cabin. If pillars are positioned rather than walls, this drawback is lifted in exchange for a heavier structure. However, this leaves the second fundamental drawback: the pillars or walls prevent an airliner to configure the cabin of the aircraft to its own desires. Due to the walls and pillars, the number of seats abreast is fixed from the moment the design is frozen. Changes in seat width, aisle width or even armrest width are prohibited, making the cabin configuration of a blended wing body as flexible as that of a narrow-body aircraft.

To circumvent these drawbacks and improve the appeal of the BWB concept to airliners, the oval fuselage concept was introduced in 2012 (Fig. 1(c)).[3] As the name suggests, the cross-section of the center section of the BWB is shaped as an oval. The oval consists of four arcs. One arc forms the upper shell (4 in Fig. 1(c)), one the lower shell (5), while at each side an arc smoothly connects to the upper and lower arcs (6 and 7). Upon pressurization, this oval wants to become a circle. To prevent this, the intersection nodes (8, 9, 13, and 14) are connected with horizontal and vertical members. The horizontal members double as floor (10) and ceiling (12), respectively, and are loaded in compression. The vertical members (17 and 18) are located close to the side arcs and are loaded in tension. In the incarnation of Fig. 1(c), the ceiling has been raised to allow for a more efficient use of the available volume. This requires additional structural members (15 and 16), which are loaded in bending, and it requires the floor member to be loaded in bending as well. In this setup, the ceiling (12) therefore also carries a bending moment. The space below the main deck can be used to store unit-load devices (19).

The implementation of the oval fuselage in the design of a blended-wing body requires a new method to estimate the weight of such a structure. This would allow a designer to make a better estimate of the (operative) empty weight (OEW) of the airplane. This is crucial in determining the impact of this technology on the overall performance of a BWB. Since a statistical database of such a fuselage structure is lacking,a weight estimation method based on structural analysis has been developed. This method is detailed in the

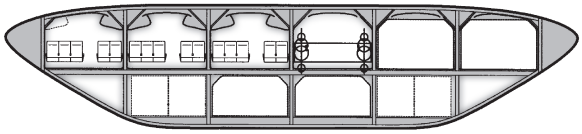

(a) The integrated skin and shell concept[1]

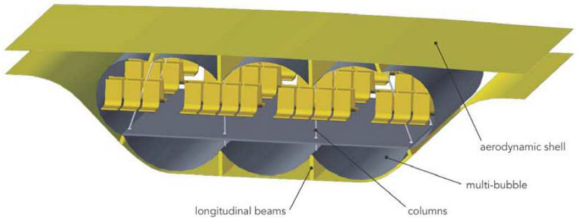

(b) The segregated pressure shell concept[2]

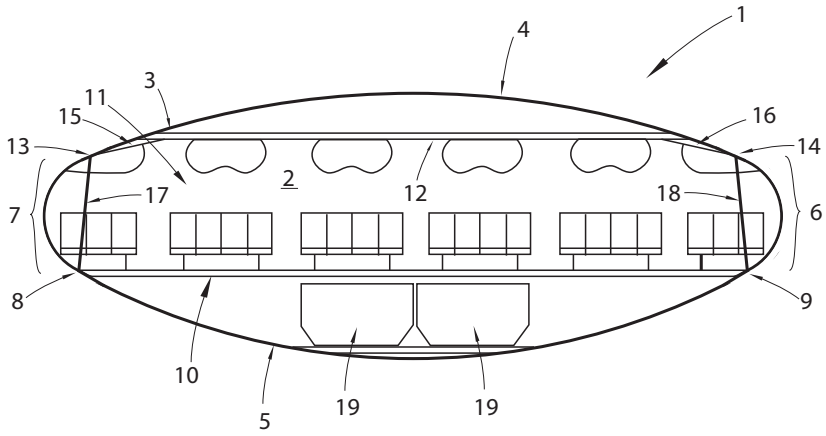

(c) The oval pressure shell concepts[3]

Figure 1.

subsequent section. This method has been implemented in an in-house airplane design tool to investigate whether the implementation of the oval fuselage in a BWB is a promising technology. We present an example of an oval-fuselage BWB in Section III.

II. Semi-Analytical Weight Estimation Method

In our treatment of the blended-wing body aircraft we follow a more traditional division of airplane components, as illustrated in Figure 2. The center body of the aircraft is mainly formed by the pressurized fuselage with oval cross section. Behind the aft pressure bulkhead a simple control surface is present that spans the width of the fuselage. The following sections present a method to estimate the weight of the entire fuselage, including control surface, cockpit, and furnishing. The structural layout is presented in Section A, followed by a discuassion of the load condition in Section B. The estimation of the structural weight of the oval fuselage is presented in Section C. The estimation of the wing weight is described in Section D. The estimation of all the remaining components is based on empirical methods and is described in Section E.

A. Primary Structure Layout and Assumptions

In Figure 3 a generic cross-section of an oval fuselage is shown. The main components and their dimensions have been indicated in the figure. The oval shell is assumed to be thin-walled with isotropic material properties. The floor and ceiling are each assumed to consist of a sandwich structure composed of a core (with thickness t_c) and two facing sheets of equal thickness (t_f) and isotropic material. The main assumption in the present method is that the thickness of each of the members is determined by the combined load of pressurization and wing bending moment (see Section B). It is assumed that the resulting structure is capable of withstanding all other loads such as passenger loads on the floor, the longitudinal loads introduced through pressurization, or the longitudinal loads introduced during a hard landing. Furthermore, it is assumed that the thickness of each of the components can be sized at each fuselage station, independent of each other. For example, the core thickness of the floor can vary from one fuselage station to the other. Finally, it has been

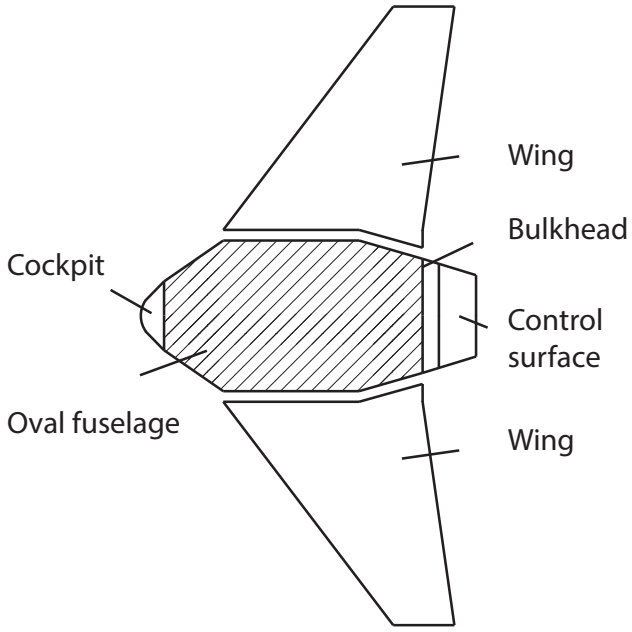

Figure 2. Schematic of the division of airplane components as followed in this paper

assumed that all materials have isotropic properties and that this structure is therefore made out of metal, rather than composite materials.

B. Loading Condition

We introduce the combined load case of pressurization (subscript p) and wing bending moment (subscript M). The loads are assumed to act on fuselage cross sections of unit length. We assume that the pressurization load is to be carried by the shells of the fuselage, and that the resultant force at the nodes where two shells meet can be decomposed in a vertical and horizontal component, to be carried by the walls and the ceiling/floor respectively. In addition to the horizontal component, we also introduce the wing bending load on the horizontal members of Figure 3. The decomposition of the loads is descibed in the following sub-sections.

1. Loads due to Pressurization

Pressurization of an enclosed volume causes hoop stresses and longitudinal stresses. From the hoop stresses we can deduce a force (F) per unit length (Δl) at the walls as a function of the differential pressure (Δp) and the inner radius of the shell (R_i):

$$\frac{F_i}{\Delta l} = \Delta p R_i \quad \text{for} \quad i = 1,\ 2,\ 3 \tag{1}$$

The resultant forces at each node can be decomposed into a force in the direction of the floor/ceiling and a force in the direction of the wall. In Figure 4 these forces are shown in each of the nodes. It can be shown that the forces in floor, ceiling and wall are related to the geometry of the oval section according to the angles β, η and ζ:

$$\frac{F_{\mathrm{ceiling}_p}}{\Delta l} = \Delta p (R_1 - R_2)\left(\cos\beta + \sin\beta \tan\zeta\right) \tag{2a}$$

$$\frac{F_{\mathrm{floor}_p}}{\Delta l} = \Delta p (R_3 - R_2)\left(\cos\eta - \sin\eta \tan\zeta\right) \tag{2b}$$

$$\frac{F_{\mathrm{wall}_p}}{\Delta l} = \Delta p (R_1 - R_2)\frac{\sin\beta}{\cos\zeta} = \Delta p (R_3 - R_2)\frac{\sin\eta}{\cos\zeta} \tag{2c}$$

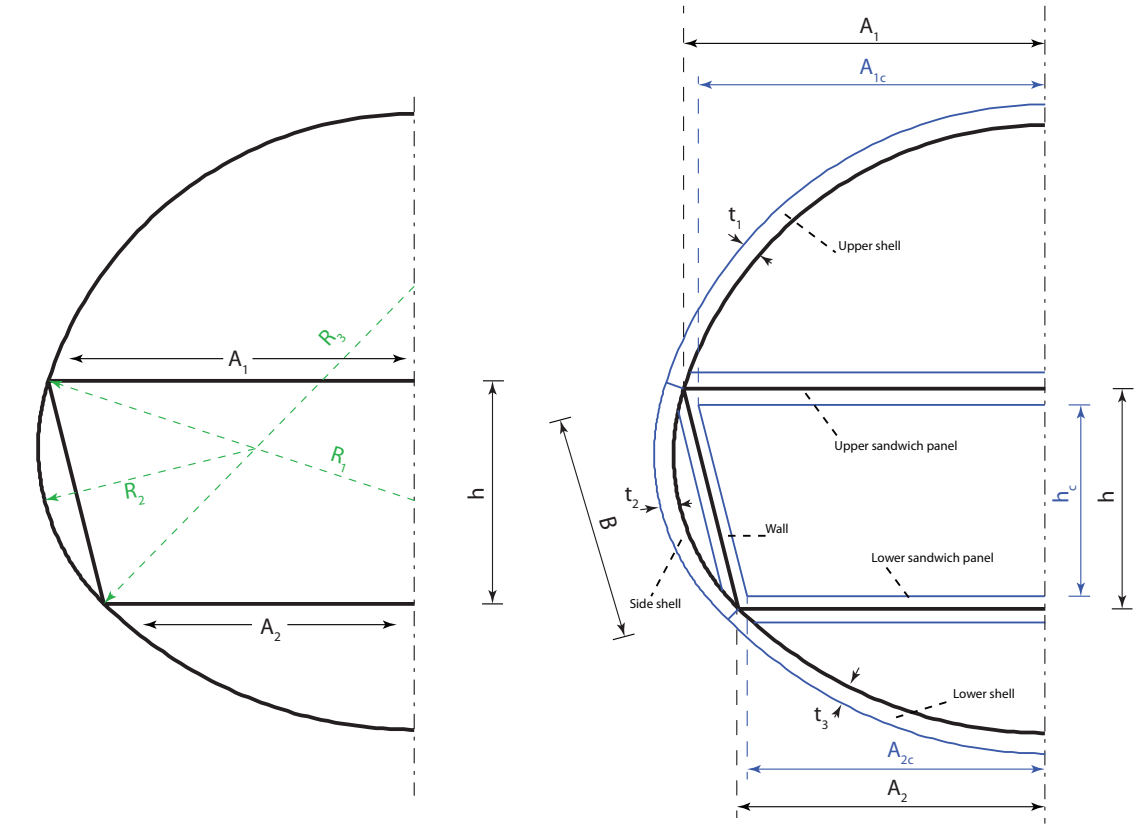

(a) Center lines of all structural components[4] (b) Structural components[4]

Figure 3. Structural layout of generic oval fuselage cross-section and relevant nomenclature

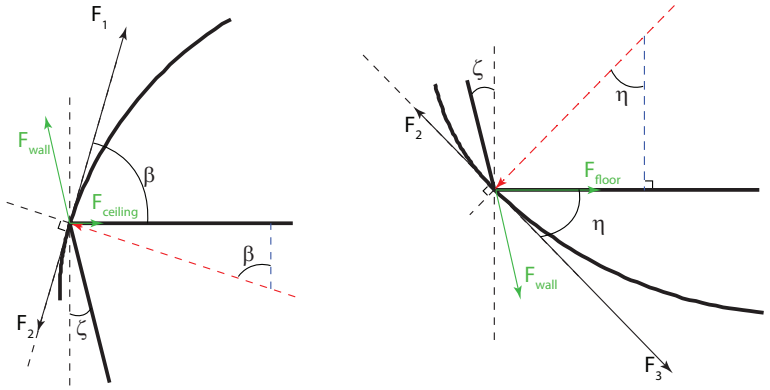

(a) Forces at the upper node[4] (b) Forces at the lower node[4]

Figure 4. Forces in floor and ceiling stemming from hoop stresses

2. Loads due to Wing Bending Moment

In Figure 5 it is shown how the wing bending moment at the root is decomposed into a force couple that introduces an axial force in the floor and ceiling. We first consider the maximum compressive force that can be introduced in the ceiling. This occurs at the ultimate load factor ($n_{\text{ult}_{\text{max}}}$), where take the assumption from Torenbeek[5] that for large commercial aircraft the maneuvre load is almost always critical, in comparison to the gust load. Hence we assumed maximum take-off weight (MTOW) to be the design condition. The compressive force in the ceiling is then a function of the root bending moment generated by the lift force

and relieved by the weight of the engines (eng) and the weight of the fuel:

$$\frac{F_{\text{ceiling}_M}}{\Delta l} = \frac{n_{\text{ult}_{\max}} \left(M_{\text{L}} - M_{\text{fuel}} - M_{\text{eng}}\right)}{hd} \tag{3}$$

Here, h is the distance between the upper and lower horizontal members and d is the wing box length at the root. If we consider the maximum compressive force in the floor, we should take the minimum ultimate load factor ($n_{\text{ult}_{\min}}$) and add the bending moments generated by fuel and engine to that. The resulting compressive force is then:

$$\frac{F_{\text{floor}_M}}{\Delta l} = \frac{-n_{\text{ult}_{\min}} \left(M_{\text{L}} + M_{\text{fuel}} + M_{\text{eng}}\right)}{hd} \tag{4}$$

These equations, (3) and (4) respectively, do not include the weight of the wing. The wing weight would impose an additional relieve for situations with positive load factor, or an additional load for negative load factors. Should the

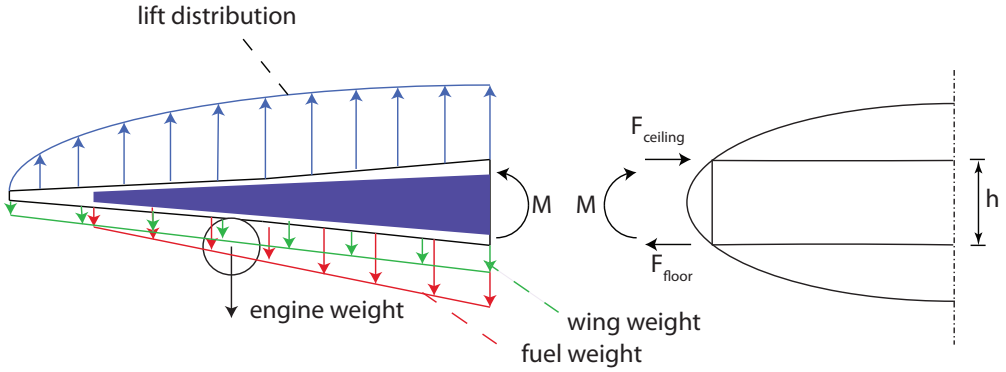

Figure 5. Wing loading causing a force couple at the wing root.

C. Weight Estimation of Primary Structure

1. Outer Shell

The outer shell forms the pressure vessel and thereby the primary structure of the fuselage, as illustrated in Figure 3(b). It is sized for pressurization loads. The thickness of the shells (t) is determined from the hoop-stress for a certain inner radius (R_{i}), assuming that this stress may not exceed the fatigue stress in tension ($\sigma_{\text{fatigue}_{\text{t}}}$) of the shell material. Imposing a safety factor j yields the following relations for the thickness of the shells:

$$t_1 = \frac{j \Delta p R_1}{\sigma_{\text{fatigue}_{\text{t}}}} \tag{5}$$

$$t_2 = \frac{j \Delta p R_2}{\sigma_{\text{fatigue}_{\text{t}}}} \tag{6}$$

$$t_3 = \frac{j \Delta p R_3}{\sigma_{\text{fatigue}_{\text{t}}}} \tag{7}$$

The mass of the shells is calculated at every fuselage station (i) of the pressurized shell. The mass of the frames to prevent general buckling instability of the shell is also accounted for. Although, the actual frame pitch is not calculated, an approach for the sizing of buckling-critical structures from NASA is adopted[6] to calculate the weight penalty due to frames. This method assumes that for buckling-critical shells, the equivalent thicknesses of the shell and frames at a certain frame spacing is $\frac{3}{4}\bar{t}$ and $\frac{1}{4}\bar{t}$, respectively. The total equivalent thickness ($\bar{t}$) of a buckling critical structure is given by:

$$\bar{t} = \bar{t}_{\text{S}_{\text{B}}} + \bar{t}_{\text{F}_{\text{B}}} \tag{8}$$

Where $\bar{t}_{\text{S}_{\text{B}}}$ is the buckling-critical thickness of the shell and $\bar{t}_{\text{F}_{\text{B}}}$ is the buckling-critical thickness of the frames. For the oval fuselage we assume that the buckling-critical thickness of the shell is equal to the previously

computed thickness to withstand pressurization. This means that the equivalent thickness of the frames is $\frac{1}{3}$ of that of the shell thickness. Therefore a factor $\frac{4}{3}$ is included when computing the mass per unit length of the top shell ($\frac{m_{\mathrm{R}_1}}{\Delta l}$), the two side shells ($\frac{m_{\mathrm{R}_2}}{\Delta l}$) and the bottom shell ($\frac{m_{\mathrm{R}_3}}{\Delta l}$):

$$\frac{m_{\mathrm{R}_1}}{\Delta l} = \frac{4}{3}\beta K_{\mathrm{lg}} K_{\mathrm{doors}} \left[(R_1 + t_1)^2 - R_1^2\right] \rho_{\mathrm{shell}} \tag{9a}$$

$$\frac{m_{\mathrm{R}_2}}{\Delta l} = \frac{8}{3}\theta K_{\mathrm{lg}} K_{\mathrm{doors}} \left[(R_2 + t_2)^2 - R_2^2\right] \rho_{\mathrm{shell}} \tag{9b}$$

$$\frac{m_{\mathrm{R}_3}}{\Delta l} = \frac{4}{3}\eta K_{\mathrm{lg}} K_{\mathrm{doors}} \left[(R_3 + t_3)^2 - R_3^2\right] \rho_{\mathrm{shell}} \tag{9c}$$

The extra thickness is disregarded in any structural calculations, as it merely serves as a mass estimate and in its equivalent form does not hold any structural significance. The additional factors $K_{\mathrm{lg}} = 1.12$ and $K_{\mathrm{doors}} = 1.25$, taken from Raymer[7] are added to account for weight penalties imposed on the shell due to cut-outs in the shell for doors, windows and landing gear. In these equations ρ_{shell} is the density of the shell material and θ is defined as: $\theta = 180[deg] - \beta - \eta$.

2. Ceiling and Floor

The floor and ceiling are modeled as sandwich panels, where the stiffness of the core is not included in the bending stiffness, making the analysis conservative. The sandwich panels are considered to be buckling critical. It is assumed that at each section the ceiling can be modeled as a perfect column, which is simply supported between the two connecting nodes at either side wall. The maximum buckling force per unit length for the first buckling mode of an unsupported member of length b, is then given by:[8]

$$\frac{F_{\mathrm{crit}}}{\Delta l} = \frac{1}{\Delta l}\frac{\pi^2 E_{\mathrm{f}} I_{\mathrm{f}}}{b^2} \tag{10}$$

Where E_{f} is the Young's modulus of the facing material and the area moment of inertia of the facings (I_{f}) is given by:

$$I_{\mathrm{f}} = \Delta l \left[\frac{1}{6}t_{\mathrm{f}}^3 + \frac{1}{2}t_{\mathrm{f}}\left(t_{\mathrm{c}} + t_{\mathrm{f}}\right)^2\right] \tag{11}$$

Where the sub-scripts f and c refer to the sandwich facing and core, respectively. Each of the equations is minimized for the mass per unit length according to the following optimization algorithm:

$$\min \quad J = 2t_{\mathrm{f}}\rho_{\mathrm{f}} + t_{\mathrm{c}}\rho_{\mathrm{c}} \tag{12a}$$

subject to:

$$F_{\mathrm{n_{ult}}} + jF_{\mathrm{h}} - F_{\mathrm{crit}} < 0 \tag{12b}$$

$$-t_{\mathrm{f}} < 0 \tag{12c}$$

$$-t_{\mathrm{c}} < 0 \tag{12d}$$

We use $F_{\mathrm{h}} = F_{\mathrm{ceiling}_p}$ and $F_{\mathrm{n_{ult}}} = F_{\mathrm{ceiling}_M}$ in case of the ceiling and $F_{\mathrm{h}} = F_{\mathrm{floor}_p}$ and $F_{\mathrm{n_{ult}}} = F_{\mathrm{floor}_M}$ for the floor. The result of this minimization is the a value for the facing thicknesses (t_{f}) and the core thickness (t_{c}). Once these thicknesses are known, the mass of the floor and ceiling can be calculated as follows:

$$\frac{m_{\mathrm{ceiling}}}{\Delta l} = 2A_1\left(2t_{\mathrm{f}_1}\rho_{\mathrm{f}} + t_{\mathrm{c}_1}\rho_{\mathrm{c}}\right) \tag{13a}$$

$$\frac{m_{\mathrm{floor}}}{\Delta l} = 2A_2\left(2t_{\mathrm{f}_2}\rho_{\mathrm{f}} + t_{\mathrm{c}_2}\rho_{\mathrm{c}}\right) \tag{13b}$$

3. Walls

The walls are sized for tension, because we assume that R_2 is always smaller than R_1 and R_3. Hence the thickness of the wall, for a unit fuselage length Δl can be related to the fatigue stress and the normal force.

$$t_{\mathrm{wall}} = \frac{jF_{\mathrm{wall}_p}}{\sigma_{\mathrm{fatigue_t}}\Delta l} \tag{14}$$

The mass of the two walls of length B is then calculated by:

$$\frac{m_{\mathrm{walls}}}{\Delta l} = 2Bt_{\mathrm{wall}}\rho_{\mathrm{wall}} \tag{15}$$

4. Total

Combining the masses of the structural components yields the total mass per unit length:

$$\frac{m}{\Delta l} = \frac{m_{\text{walls}}}{\Delta l} + \frac{m_{\text{ceiling}}}{\Delta l} + \frac{m_{\text{floor}}}{\Delta l} + \frac{m_{\text{R}_1}}{\Delta l} + \frac{m_{\text{R}_2}}{\Delta l} + \frac{m_{\text{R}_3}}{\Delta l} \tag{16}$$

The total mass of the primary structure is obtained by summing the weight of each section over all fuselage stations oval cross sections:

$$m = \int_{\text{begin}}^{\text{end}} \frac{m}{\Delta l} \mathrm{d}x \tag{17}$$

D. Wing Weight

The weight of the outer wing is calculated by implementing the Class-II.5 wing weight prediction of Torenbeek[5] on the wing sections of the BWB spanning from the edge of the oval fuselage to the wing tip. These are the sections labeled "Wing" in Figure 2. The wing weight is computed as the sum of functional components of the wing structure, where the basic weight required to resist bending and shear loads is computed from the spanwise material distribution. Weight penalties are imposed to account for non-optimum effects, such as aeroelastic effects. The Torenbeek method is based on several assumptions, most importantly that all loads will be ultimately concentrated in the primary wing structure, consisting of upper and lower stiffened panels, front and rear spar and ribs. Also constant sweep angle over a section is assumed. Furthermore the structure is assumed a statically determined equivalent system, where bending is absorbed only by the stiffened panels and spar flanges and spar webs take the shear loads. Simple beam theory is used for the analysis. Torsion is not taken into account explicitly and only maneuvering and gust loads are considered as determining cases. To account for the non-ideal situation, correction factors are applied. For more detail please refer to the original manuscript.[5] The method has been extended by incorporating bending relief of concentrated masses of the fuel load and engines, as proposed by Torenbeek himself.[5]

E. Weight Estimation of Secondary Structure and Non-Structural Items

The weight estimation of secondary structure and non-structural items is detailed in the this section. These items are additional to the previously calculated weights of the wing and center-fuselage primary weight, all together forming the operative empty weight (OEW) of the BWB. The secondary structure and non-structural items are calculated using the Torenbeek Class-II weight estimation.[9] Yet, since this method is not specific for BWB aircraft and contains some information that can be considered out-dated by the current state-of-the-art, some BWB specific estimates or updated information is used. Some estimates specifically for blended wing body aircraft by Howe[10] have in this case been implemented. Only the additions to, and modifications of, the Torenbeek method[9] are described in this section.

1. APU

The installed mass of the auxiliary power unit (APU) is related to the dry-mass the APU. The PW980 APU of the Airbus A380 is used as a reference. In addition, the A380 APU is estimated to be 10% larger than the PW901a of the Boeing 747-400.[11] The PW901a weighs 835 lbs according to information from Virginia Tech.[12] The installed weight can be calculated according to the Torenbeek method[9] using this dry-mass for the APU.

2. Radar

The mass of the radar is estimated from that of a typical Honeywell weather radar for commercial aircraft, the Primus 880,[13] at 20kg.

3. Paint

Based on a press release by Airbus for the A380,[14] the weight of the paint is estimated at 0.3kg per square meter wetted area.

$$W_{\text{paint}} = 0.3 \cdot S_{\text{wet}} \quad [kg] \tag{18}$$

4. Flightdeck Furnishing

From the weight of pilot and fold-away seats from Torenbeek,[9] the weight of the flightdeck furnishing is rounded upwards to 200kg to account for the rest of the furnishing.

5. Cabin Furnishing

Roskam[15] provides the mass of the cabin furnishing, including toilets and galleys and overhead luggage compartments for the Boeing 747-100. This is divided equally over the cabin surface of this aircraft to obtain a ratio of 51.5kg furnishing per square meter of cabin area. This specific aircraft is used as a reference as it is capable of transporting 400+ passengers in a 2 class configuration and, most importantly, because of the availability of this rare reference data of the furnishing weight in Roskam.[15]

6. Crew

Flight crew and cabin crew cannot be considered equipment, however, they are commonly included in the OEW, as they are vital to the operation of the aircraft. The original anthropological data from 1982[9] has been adapted to better match the average human in 2013. This weight has been considered for both the flight crew and cabin crew, including there luggage, and it is set to 93kg per crew member, including luggage.

7. Cargo Containers

The weight of cargo containers, on the lower deck of the aircraft, must be considered in the operational items. The LD-3 tare weight of 72kg each, as used by British Airways World Cargo[16] is used in the analysis.

8. Fuselage Trailing Edge

The weight estimation of the fuselage section has been described earlier, however this does not include the nose cone or the section aft of the passenger cabin. The weight of the trailing edge that completes the aerodynamic shape of the wing, based on the planform area of the trailing edge is calculated according to the following relation from Torenbeek:[5]

$$W_{\mathrm{fus_{TE}}} = S_{\mathrm{TE}} \left[60 \left(1 + 1.6 \cdot \sqrt{\frac{W_{\mathrm{TO}}}{10^6}} \right) + \Delta \right] \quad [kg] \tag{19}$$

A similar approach is adapted here, the trailing edge is assumed to only complete the aerodynamic shape of the wing. It is assumed that the trailing edge section can be used as a control surface as well, as is modeled in the previous equation by Δ. This resembles the complexity of the flap system present on the trailing edge of a wing, so, for a control surface, a single slotted flap is assumed to bear the most resemblance to an elevator. Therefore $\Delta = 0$, from Torenbeek.[5]

9. Nose Cone Shell

Because of the specific shape of the BWB, the weight of the nose cone shell, which is not included in the mass prediction of the fuselage, is calculated with an equation from the BWB weight estimation method of Howe.[10] In this equation, B is the maximum with of the nose cone in meters, S_{nc} is the nose cone wetted area in m^2, where an ellipsoidal dome is assumed, the maximum pressure differential δ_{p} in bar and $\bar{f}_{\mathrm{t}}$, which is the ratio of the maximum working stress to 10^8. In this case the fatigue stress in tension at $100,000$ cycles is used for the maximum working stress. ρ_{mat} is the material density of the shell.

$$W_{\mathrm{nc}} = 1.2 \frac{B \cdot S_{\mathrm{nc}} \cdot \Delta_{\mathrm{p}} \cdot \rho_{\mathrm{mat}}}{\bar{f}_{\mathrm{t}}} \times 10^{-3} \quad [kg] \tag{20}$$

10. Crew Floor

With a BWB specific nose cone, also the crew floor mass equation is taken from Howe, where S_{CF} is the area of the crew floor in m^2.

$$W_{\mathrm{cf}} = (7 + 1.2B) \cdot S_{\mathrm{CF}} \quad [kg] \tag{21}$$

11. Windscreen

Also the mass of the windscreen is estimated according to the equation by Howe, where S_{WS} is the windscreen area in m^2 and V_{D} is the dive speed in m/s.

$$W_{\mathrm{ws}} = 0.75 \cdot S_{\mathrm{WS}} \cdot V_{\mathrm{D}} \cdot \Delta_p \ \ [kg] \tag{22}$$

12. Front Pressure Bulkhead

The front pressure bulkhead is not included in the fuselage weight estimation and is also estimated according to Howe.[10] S_{fpb} is the area of the bulkhead in m^2 where a dome shape is assumed, hence $\bar{h}_{\mathrm{fpb}} = 1$ and ρ_{mat} is the material density in $\mathrm{kg/m}^3$.

$$W_{\mathrm{fpb}} = 6.5 \cdot \bar{h}_{\mathrm{fpb}} \cdot S_{\mathrm{fpb}} \cdot \Delta_{\mathrm{p}} \cdot \rho_{\mathrm{mat}} \times 10^{-3} \ \ [kg] \tag{23}$$

13. Rear Pressure Bulkhead

The mass of the rear pressure bulkhead is estimated similar to that of the front pressure bulkhead, where S_{rpb} is calculated as the surface within the last fuselage section in m^2. Here a flat bulkhead is assumed, hence $\bar{h}_{\mathrm{rpb}} = 1.25$.

$$W_{\mathrm{rpb}} = 6.5 \cdot \bar{h}_{\mathrm{rpb}} \cdot S_{\mathrm{rpb}} \cdot \Delta_{\mathrm{p}} \cdot \rho_{\mathrm{mat}} \times 10^{-3} \ \ [kg] \tag{24}$$

14. Cargo Floor

The upper and lower horizontal sandwich members fulfill a double function as an upper cargo floor and cabin floor, however, the cargo floor for the lower deck is not computed yet. Therefore the following equation from Howe[10] is used:

$$W_{\mathrm{frf}} = 2.6\,(1 + 0.6 B_{\mathrm{frf}}) \cdot S_{\mathrm{frf}} \cdot \rho_{mat} \times 10^{-3} \ \ [kg] \tag{25}$$

Here B_{frf} is the maximum width of the cargo floor in m and S_{frf} is the surface area of the cargo floor in m^2.

III. Conceptual Design Study: 400 Passenger BWB Aircraft

The present section presents an example where the oval fuselage has been integrated in a BWB aircraft. The goal of this section is to find out whether the implementation of the oval fuselage in a BWB aircraft is worthwhile to further investigate. A design study such as presented in this section could reveal for example a large operative empty weight (OEI) which would trump the advantages discussed in the introduction of this paper. An in-house design tool has been modified to include the empty weight estimation of the oval fuselage. The top-level requirements for this example aircraft are comparable to a Boeing 777-200LR (see Section A). The main characteristics of the design tool are described in Section B. The resulting design is presented in Section C along with key design characteristics.

A. Top-Level Requirements

A selection of the most important design requirements are presented in the list below:

- Number of passengers: 400 (350 economy, 50 business)
- Additional cargo: 20,000kg
- Harmonic Range $15,200$km
- Take-off distance: < 2500m
- Landing distance: < 2500m
- Stall speed clean configuration: < 70m/s
- Stall speed take-off configuration: < 80m/s
- $C_{n_\beta} > 0$
- $C_{l_\beta} < 0$
- Static stability margin: $\frac{x_{\mathrm{ac}} - x_{\mathrm{cg}}}{c} > 0.05 \quad \forall \quad x_{\mathrm{cg}}$

- Load on nose gear: $5\% < F_{\text{nose}} < 20\%$
- Max span and length: 80m
- Airworthiness Regulations: FAR/CS 25

The requirements bear resemblance to those for the Boeing 777-200LR[17] which has a harmonic range of 13,900km with a 301 passenger three class cabin, or re-configured with a 400 passenger two-class cabin (as in the Boeing 777-200ER). In addition to the requirements, the following configuration was selected: Aft swept wings, 4-engines, engines mounted under the wing, winglets doubling as twin vertical tails, two main gear struts, a single nose strut. Important to note is the required static margin for the aircraft of at least 5% and that the airplane is required to carry an additional 20,000kg payload in addition to the passengers and their luggage.

B. Design Procedure

The configurational choice of aft swept wings, 4-engines mounted under the wing and winglets doubling as twin vertical tails is translated into 19 design variables. These 19 variables describe the shape of the center body (6 variables) as well as the outer wing (12 variables), which is divided in two parts. The height of the vertical tail contains the last design variable. Each of these design variables has been given an upper and lower bound. A gradient-based optimization algorithm alters these variables between these bounds in order to find the maximum harmonic range.

A preliminary sizing of wing area, thrust and maximum take-off weight is carried out. The airplane is subsequently analyzed by the following analysis tools: aerodynamic analysis, cabin volume analysis, estimation of weight and balance, stability analysis, trim analysis, and performance analysis. A full description of the design method can be found in Vos and Van Dommelen (2012).[18] For the airframe analysis of the center body, we need to make assumptions on the various constants that appear in the equations of Section II. We have listed those constants in Table 1. The material of choice is Aluminum (AL7075T6). The value of $\sigma_{\text{fatigue}_t}$ is based on the maximum stress after 10^5 cycles.

Table 1. Assumed values for the weight estimation

constant	value	unit
j	1.5	˜
Δp	$80,000$	N/m^2
$\sigma_{\text{fatigue}_t}$	$156 \cdot 10^6$	N/m^2
ρ_{shell}	$2,800$	kg/m^3
ρ_c	52	kg/m^3
ρ_f	$2,800$	kg/m^3
E_f	$72.5 \cdot 10^9$	N/m^2
$n_{\text{ult}_{\text{min}}}$	$1.5 \cdot -1$	˜
$n_{\text{ult}_{\text{max}}}$	$1.5 \cdot 2.5$	˜

C. Results and Discussion

The result of the design optimization is a BWB of which the 3-views are shown in Figure 6. The airplane measures 70m in span and almost 46m in length. The oval fuselage section can be observed clearly in the front view of the airplane. Note that the radius of the side-shell is constant over the entire centerbody and that part of it protrudes into the outer wing. A second important characteristic is the high wing sweep. The outer wing has a leading edge wing sweep of 47°. This is due to the required stability margin of 5%. The high sweep angle also allows a thicker section of the outboard wing. At the kink of the most outboard wing section, the thickness-to-chord ratio in streamwise direction amounts to 12%. This decays to 10% at the wing tip.

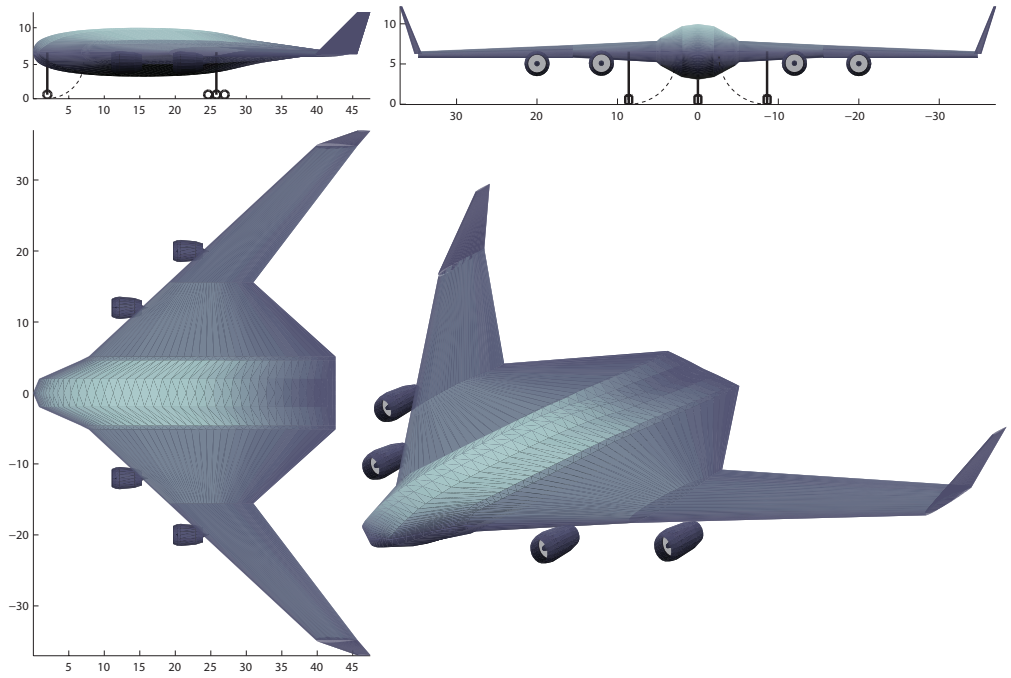

Figure 6. Three-view of 400-passenger BWB (dimensions in meters).

The following characteristics were obtained:

- MTOW= 395 ton
- Harmonic range: $15.2 \cdot 10^3$ km
- $L/D|_{\max}$: 26.6
- $L/D|_{\text{average}}$: 26.3
- Fuel consumption over harmonic range: 2.05 kg/pax/100km

We put these numbers in perspective, by loosely comparing the aircraft to the Boeing 777-200LR. This aircraft has a harmonic range of $13.9 \cdot 10^3$km when configured to carry maximum payload. This shows that the BWB has a harmonic range that is approximately 9% larger, with a similar fuel consumption. However, the BWB also has a 13.5% higher MTOW than the 777-200LR (395 ton compared to 348 ton for the 777-200LR. This already suggests that the structural efficiency of the BWB may not be as high as would be expected.

A selection of the airplane's weight breakdown is shown in Figure 7. The ratio between OEW and MTOW amounts to 45%, for comparision the 777-200LR has an OEW fraction of 41%. This indicates that the structural efficiency of the BWB is not on par with conventional aircraft. As can be seen from Fig. 7(c), the fuselage airframe (including cockpit and trailing edge) amounts to 47.3 tons (26% of OEW). The center fuselage barrel comprises of the six elements of Equation (16). These elements are shown in Figure 7(d). We can see that the bottom and top shell have the same weight, due to the symmetry of the cabin. Furthermore, the floor and ceiling are large contributors to the weight. The floor is somewhat lighter due to the lower negative aerodynamic load factor that was accounted for in (3) and (4), respectively. The weight of the vertical walls and the two side shells is relatively low (each 3% of the total barrel weight).

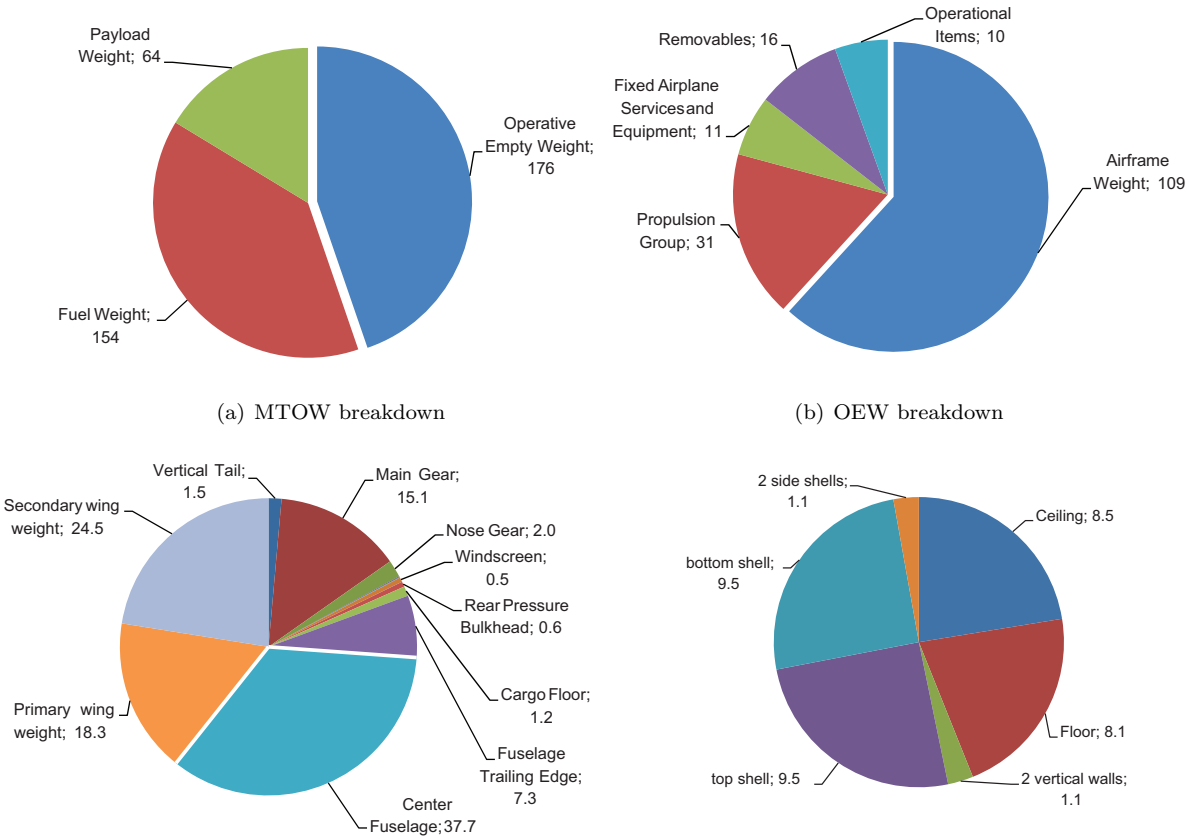

(a) MTOW breakdown

(b) OEW breakdown

(c) Airframe weight breakdown

(d) Center fuselage breakdown

Figure 7. Breakdown of characteristic weights for BWB of Figure 6 (all weights in metric tons).

If we overlay the plan view and side view of this BWB and the Boeing 777-200LR (Figure 8) we intuitively feel that the BWB is oversized. It clearly has a much larger planform area than the triple seven, which would contribute to a higher friction drag. The reason why the wing is so big does not stem from the requirements on field performance. The landing distance (2100m) and the take-off distance (1500m) are still far away from the constraints. Also the stall speeds are well below what is required. The only requirements that are active in this design are the cabin floor area and the minimum static margin (5% MAC). It is therefore hypothesized that the cabin floor area has a (too) large impact on the wetted area of the BWB. The relatively large lift-to-drag ratio that has been quoted above is mainly due to the large span. As is demonstrated in Rettie (1983),[19] the lift-to-drag ratio at $ML/D|_{\max}$ is a function of $b/\sqrt{S_{\text{wet}}}$. In other words, the lower induced drag is offsetting the increase in friction drag, resulting in a relatively high lift-to-drag ratio. With a wetted area of 2700m^2 and a span of 70 meters, the value of $b/\sqrt{S_{\text{wet}}} = 1.34$ for this blended wing body. If we follow the analysis of Rettie, a maximum lift-to-drag ratio of only 22 would be expected, based on an average friction coefficient of 0.003. This indicates that we should treat the L/D-values quoted above with some reservation.

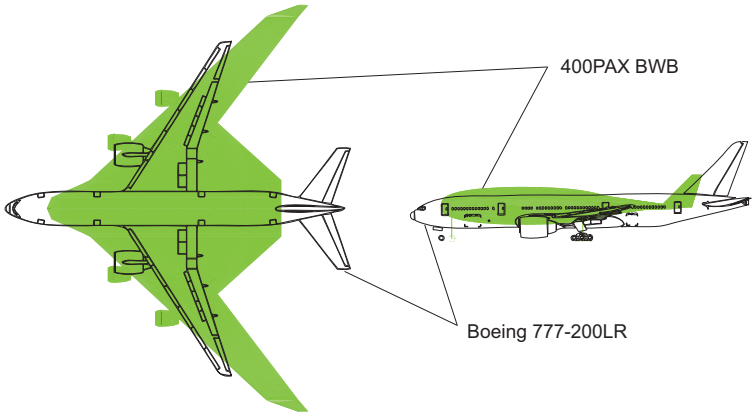

Figure 8. Comparison between BWB and Boeing 777-200LR.

IV. Conclusions and Future Research

This paper presents a semi-analytical weight estimation method for fuselages with oval cross-section, specifically for a BWB aircraft with an oval-fuselage. This weight estimation method is based on a structural analysis of the oval-fuselage and is implemented in an in-house airplane design tool to investigate whether the oval fuselage is a promising technology for BWB aircraft. A 400-passenger BWB with an oval fuselage has been designed for a harmonic range of 15,200km, while having a stability margin of 5%. Through this analysis a MTOW of 395 metric tons was found for this harmonic range, with a fuel consumption of 2.05kg/pax/km. The analyis shows an OEW fraction of 45%, which is slightly larger than that of a comparable aircraft, such as the Boeing 777-200LR. This means that the BWB is not necessarily structurally more efficient than conventional aircraft.

In future work the weight estimation methodology will be further detailed and validated by means of finite element analysis methods. Moreover the wing-fuselage intersections and load transfer between the structural elements at this location will be included in future structural analysis. In order to verify the developed methodology, the structural analyis will be validated by, means of a thorough analysis of the load cases that are currently used for the sizing. This means considering for example take-off and landing loads, as well as the loads introduced on the floor and ceiling panels by the cargo and passenger cabin. In addition to this, the sizing of the floor and ceiling to cope with the force couple that is introduced by the wing bending moment will be detailed, by including the wing bending relief. Furthermore, the load case that is used here will also be reconsidered. This means including the load condition at maximum zero fuel weight, including the gust load factor. Moreover, the high L/D ratio that is found will be challenged by reconsidering the aerodynamic analysis.

Acknowledgements

The authors would like to thank the great insight and advice of Dr. Francois Geuskens and the valuable contributions of mr. Kristian Schmidt.

References

[1]Liebeck, R. H., "Design of the BlendedWing Body Subsonic Transport," *Journal of Aircraft*, Vol. 41, No. 1, January-February 2004, pp. 10–25.

[2]Geuskens, F. J. J. M. M., Bergsma, O. K., Koussios, S., and Beukers, A., "Pressure Vessels & Pressure Cabins for Blended Wing Bodies," *ICCM-17 17th International Conference on Composite Materials 27 Jul 2009 - 31 Jul 2009, Edinburgh International Convention Centre (EICC), Edinburgh, UK*, 2009, pp. 1–12.

[3]Vos, R., Geuskens, F. J. J. M. M., and Hoogreef, M. F. M., "A New Structural Design Concept for Blended Wing Body Cabins," *53rd AIAA/ASME/ASCE/AHS/ASC Structures, Structural Dynamics and Materials Conference, Honolulu, Hawaii*, Apr. 23-26, 2012.

[4]Hoogreef, M. F. M. and Vos, R., "The Oval Fuselage: A New Structural Design Concept for Blended Wing Body Cabins," *3rd Aircraft Structural Design Conference, 9-11 October 2012, Delft University of Technology, The Netherlands*, 2012.

[5]Torenbeek, E., "Development and Application of a Comprehensive, Design-sensitive Weight Prediction Method for Wing Structures of Transport Category Aircraft," Tech. rep., Delft University of Technology, Faculty of Aerospace Engineering, 1992, Report LR-693.

[6]Ardema, M. D., Chambers, M. C., Patron, A. P., Hahn, A. S., Miura, H., and Moore, M. D., "Analytical Fuselage and Wing Weight Estimation of Transport Aircraft," Tech. Rep. TM 110392, National Aeronautics and Space Administration, May 1996.

[7]Raymer, D. P., *Aircraft Design: A conceptual approach*, American Institute of Aeronautics and Astronautics, Inc., Washington, DC, 1992.

[8]Ashby, M. F., *Materials Selection in Mechanical Design*, Butterworth-Heinemann, Oxford, UK, 3rd ed., 2005.

[9]Torenbeek, E., *Synthesis of Subsonic Airplane Design*, Delft University Press, Kluwer Academic Publishers, 1982.

[10]Howe, D., "Blended wing body airframe mass prediction," *Proceedings of the Institution of Mechanical Engineers, Part G: Journal of Aerospace Engineering*, Vol. 215, 2001, pp. 319–331.

[11]Anonymous, *Thrust advance*, Flight International, 20-26 May 2003, A380-special pages 23-25.

[12]Anonymous, *Secondary Power Systems*, Virginia Tech, In-house, Accessed 22 May 2012, Lecture Slides `http://www.dept.aoe.vt.edu/~mason/Mason_f/SecondaryPwrSys.ppt`.

[13]Anonymous, *Honeywell Primus 880 Weather Radar*, Accessed 16 May 2012, `http://www.honeywell.com/sites/servlet/com.merx.npoint.servlets.DocumentServlet?docid=D59602700-804D-8E92-87FC-22F9AEF5819E`.

[14]Anonymous, *Airbus starts painting first A380 for Singapore Airlines*, Airbus S.A.S., 11 April 2007, Accessed 28 May 2012, Press Release `http://www.airbus.com/en/presscentre/pressreleases/pressreleases_items/07_04_11_A380_first_paint.html`.

[15]Roskam, J., *Airplane Design*, Roskam Aviation and Engineering Corporation, 1985.

[16]Anonymous, *Unit Load Devices*, British Airways World Cargo, 2012, Accessed 24 March 2012, `http://www.baworldcargo.com/configs/BAWCconfigurations.pdf`.

[17]Anonymous, *777-200LR Airplane Characteristics for Airport Planning*, Boeing Commercial Airplanes, May 2011.

[18]Vos, R. and van Dommelen, J., "A Conceptual Design and Optimization Method for Blended Wing Body Aircraft," *Proceedings of 53rd AIAA/ASME/ASCE/AHS/ASC Structures, Structural Dynamics and Materials Conference*, AIAA 2012-1756, Honolulu, HI, 23-26 April 2012.

[19]Rettie, I. H., "Aerodynamic Design for overall verhicle perfromance," *AGARD-R-712 - Special Course on Subsonic/Transonic Aerodynamic Interference for Aircraft*, AGARD, 1983.